Plasmonics (2009) 4:153–159
DOI 10.1007/s11468-009-9086-2

Unidirectional Surface Plasmon Polariton Excitation on Single Slit with Oblique Backside Illumination

Hwi Kim · Byoungho Lee

Received: 19 September 2008 / Accepted: 25 February 2009 / Published online: 17 March 2009

Abstract We have theoretically investigated the unidirectional surface plasmon polariton (SPP) excitation on single slits with oblique backside illumination. An aperture diffraction method is devised, from which the conditions of slit width and beam illumination angle for the unidirectional SPP excitation are formulated analytically. The derived unidirectional conditions are validated with vectorial electromagnetic simulation using the rigorous coupled wave analysis.

Keywords Surface plasmon polariton · Unidirectional excitation · Rigorous coupled wave analysis

Introduction

Recently, surface plasmon polariton (SPP) subwavelength optics, i.e., plasmonics, is advancing fast. SPP-based information processing at the nano-scale dimensions is considered a promising technology to overcome limitations of the present electronics-based information technologies [1–3]. Novel concepts and methods have been developed to solve challenging problems. SPP has great potential in other areas such as bio-photonics and meta-materials as well as information technologies.

Many aspects of SPP have been intensively researched to exploit full potentials of SPP. The efficient excitation method of SPP is one of fundamental issues in plasmonics. Since SPP is a low-dimensional electron-electromagnetic coupled surface wave that exists at a metal/dielectric interface [3], various methods using total internal reflection (TIR), nano tips, grating diffraction, and subwavelength slits have been developed to generate necessary SPP momentum in exciting SPPs [4].

Functional excitation methods of SPP using nanostructures having more complex features than the basic configurations are interesting research issues. Recently, the unidirectional excitation of SPP on localized structures was studied by some authors [5, 6]. Basically, the unidirectional excitation of SPP can be observed in the Kretschmann configuration using TIR. However, to implement SPP devices and systems at the nano dimensions, local SPP excitation localized on a subwavelength region is necessary. The simplest configuration of local SPP excitation is using subwavelength single slits. The SPP excitation on single slits has been researched due to its fundamental importance [7, 8] and application potentials [5, 9, 10] as a localized SPP source. Regarding the unidirectional SPP excitation on localized structures, it was reported that surface Bragg grating can be used for the efficient unidirectional excitation [5] and slanted surface dielectric grating structures can produce efficient unidirectional SPP excitation via volume diffraction effect [6].

In this paper, we show that oblique incidence beams on single slits excite the unidirectional SPPs. To understand this effect, an aperture diffraction model is devised, from which the conditions of slit width and beam illumination angle for the unidirectional SPP excitation are analytically formulated. Using the rigorous coupled wave analysis (RCWA) [9–11], the derived unidirectional excitation conditions are comparatively examined with vectorial electromagnetic analysis results.

H. Kim · B. Lee (✉)
National Creative Research Center for Active Plasmonics Application Systems, Inter-University Semiconductor Research Center and School of Electrical Engineering,
Seoul National University,
Gwanak-Gu Gwanakro 599,
Seoul 151-744, Korea
e-mail: byoungho@snu.ac.kr

In the "Surface plasmon polariton excitation on a single slit with oblique backside illumination" section, the unidirectional SPP excitation on a single slit is observed within the framework of the RCWA modeling. In the "Theoretical analysis of the excitation of surface plasmon polaritons on single slits" section, theoretical analysis on its physical origin is described. In the last section, concluding remarks are given.

Surface plasmon polariton excitation on a single slit with oblique backside illumination

The SPP excitation on single slits is one of basic geometries in plasmonics. In most previous works on this geometry, the backside illuminating beam has been assumed to be a normal incident beam. However, when the illuminating beam is oblique, the SPP is excited asymmetrically along the right and left directions. Figure 1 illustrates a schematic of SPP excitation on a single slit with an oblique backside illumination. The slit width and the metal film thickness are denoted by *w* and *t*, respectively. Let us first observe the SPP excitation on a single slit within the RCWA framework. The free space wavelength of the illumination plane wave is set to 650 nm and the permittivity values of the metallic (Au) film and air at this wavelength are $\varepsilon_m(=-9.5487+j1.1327)$ and $\varepsilon_a(=1)$, respectively. In the situation shown in Fig. 1, the excitation strength of the leftward SPP, J_L, and the rightward SPP, J_R, are expected to be significantly different because of the asymmetry of the illuminating beam. Furthermore, we can expect that at a certain condition, the excitation strength of the leftward SPP, J_L, may be almost zero, so, as a result, the unidirectional excitation of the rightward SPP, J_R, is observed.

Figures 2 and 3 show the RCWA results of the normal and oblique backside illuminations on the slit with film thickness, *t*, of 300 nm and slit width, *w*, of 730 nm. In this RCWA simulation, the incident plane wave with an incidence angle of θ is represented by

$$\mathbf{U} = (\cos\theta\mathbf{x} - \sin\theta\mathbf{z})\exp(jk_0(\sin\theta x + \cos\theta z)), \quad (1)$$

where k_0 is a free space wavenumber given by $k_0=2\pi/\lambda$ and λ is a free space wavelength of 650 nm. The total number of *x*-direction Fourier spatial harmonics is set to 161, which is the number of spatial harmonics showing a reasonable convergence, and the *x*-direction supercell period, L_x, is chosen to be 15 μm. The perfect matched layer (PML) model adopted in [9] is used in the RCWA.

In Fig. 2(a) and (b), the *x*-directional and *z*-directional electric field distributions are shown, respectively, where we can consider the *z*-directional electric field to indicate the excited SPP. As seen in Fig. 2(b), the leftward SPP, J_L, and rightward SPP, J_R, are excited symmetrically. The excitation strength of J_L and J_R are exactly the same. Figure 3 shows the RCWA result in the case of the oblique

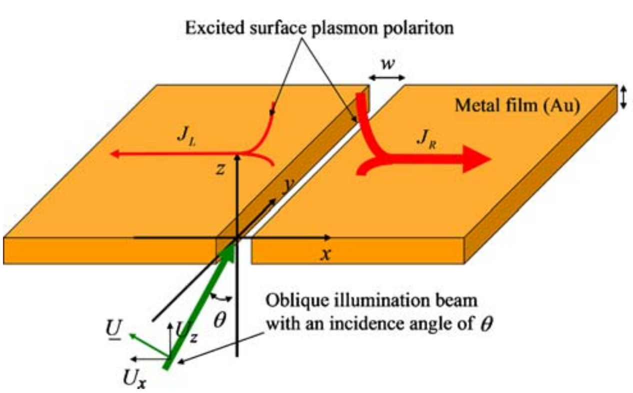

Fig. 1 Asymmetric excitation of the rightward SPP, J_R, and the leftward SPP, J_L, on a single slit with an oblique backside illumination

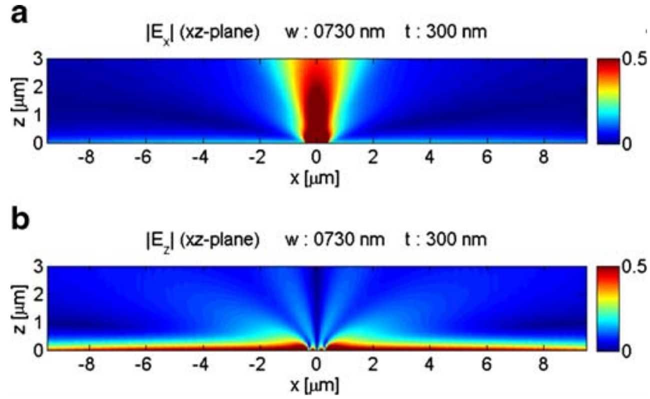

Fig. 2 RCWA result of normal incidence on a slit sample with metal film thickness of 300 nm and slit width of 730 nm: **a** *x*-directional electric field distribution and **b** *z*-directional electric field distribution

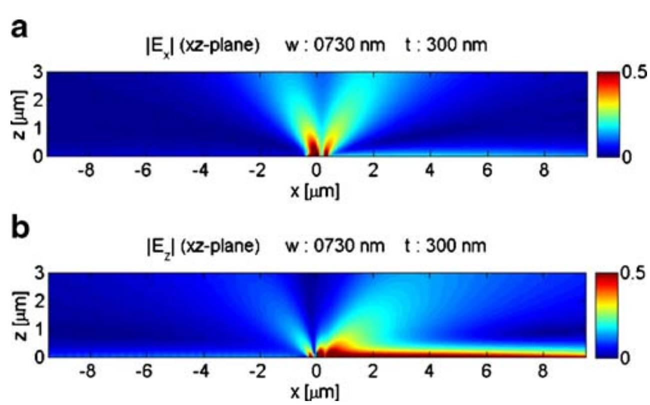

Fig. 3 RCWA result of oblique incidence (θ=55°) on the same slit sample: **a** *x*-directional electric field distribution and **b** *z*-directional electric field distribution

backside illumination with the incidence angle of 55° on the same slit. The x-directional and z-directional electric field distributions are shown, respectively, in Fig. 3(a) and (b). In this case, as seen in Fig. 3(b), the unidirectional SPP toward the right direction is observed. The excitation strength of J_{L} is significantly smaller than that of J_{R}.

Theoretical analysis of the excitation of surface plasmon polaritons on single slits

In this section, a theoretical analysis on the unidirectional SPP excitation phenomenon demonstrated in the previous section is described. For the theoretical analysis on the excitation of SPP on single slits, we employ a comparative analysis approach using two feasible aperture diffraction models having subtle difference in the aperture model. Figure 4(a) and (b) illustrate the aperture diffraction models of a single slit with finite thickness, t, and slit width, w, illuminated by an oblique incidence beam. In the aperture diffraction model shown in Fig. 4(a), the thickness of the metal film is ignored, thus the incident beam illuminates the aperture on the front side of the metal film uniformly. This model is a classical model adopted in the scalar diffraction theory of Fourier optics. In the aperture diffraction model shown in Fig. 4(b), the shadow effect caused by the sidewall with finite thickness is carefully taken into account as an important factor in the diffraction analysis. The concept of the shadow effect is hinted from Sommerfeld's half-infinite perfect conductor diffraction problem [12]. In this case, the thickness of the metal film, t, and the edge diffraction angle, Ψ, become important factors. It is noted that, in the case of normal incidence, two models become the same since the sidewall shadow disappears.

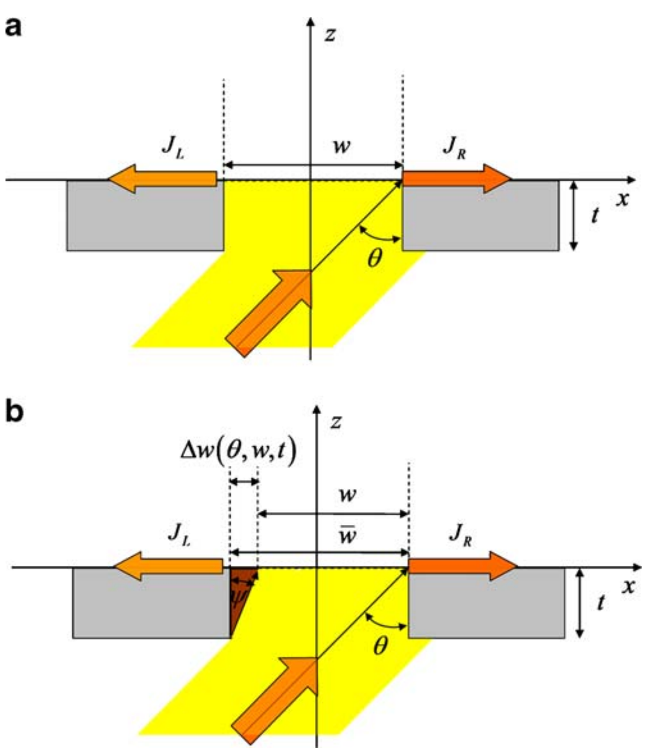

Fig. 4 **a** Simple aperture diffraction model in the scalar diffraction theory of Fourier optics, **b** aperture diffraction model including the shadow effect, where the shadow effect caused by the left sidewall of the slit with finite thickness, t, is taken into account

By the comparative analysis of two models, we can eventually obtain a phenomenological understanding on the physical origin of the unidirectional SPP excitation. As the first step, let us describe the scalar diffraction theory of the obliquely incident beam by the slit based on the first model shown in Fig. 4(a). Let the slit aperture be represented by the rectangle function, $\Gamma(x)$,

$$\Gamma(x) = \begin{cases} 1 \ \text{for} |x| \leq w/2 \\ 0 \ \text{for} |x| > w/2 \end{cases} . \tag{2}$$

Let us assume that the apertured optical field profile at the slit illuminated by the oblique beam is given by $\Gamma(x)\exp(jk_0 \sin\theta x)$, then the angular spectrum of the apertured optical field, $\Pi(\alpha)$, is obtained by

$$\begin{aligned}\Pi(\alpha) &= \int_{-\infty}^{\infty} \Gamma(x)\exp(jk_0\sin\theta x)\exp(-j2\pi\alpha x)dx \\ &= w\mathrm{sinc}\left[\left(\frac{\sin\theta}{\lambda} - \alpha\right)w\right],\end{aligned} \tag{3}$$

where α is spatial-frequency and sinc(x) is defined by sinc (x)=sin(πx)/(πx). $\Pi(\alpha)$ is a shifted form of the structural angular spectrum of the aperture rectangle function, $\Gamma(x)$. Let us define the spatial-frequency of SPP wave, α_{SPP}, by

$$\alpha_{\mathrm{SPP}} = \mathrm{real}\left[\frac{1}{\lambda}\sqrt{\frac{\varepsilon_a\varepsilon_m}{\varepsilon_a + \varepsilon_m}}\right] = \frac{1}{\lambda_{\mathrm{SPP}}}, \tag{4}$$

where ε_{a} and ε_{m} are the permittivity values of air and metal film, respectively. real[a] is the real part of a complex number a. Let us assume that the angular spectrum components at α_{SPP} and -α_{SPP}, i.e., $\Pi(\alpha_{\mathrm{SPP}})$ and $\Pi(-\alpha_{\mathrm{SPP}})$, contribute to the excitations of rightward SPP, J_{R}, and leftward SPP, J_{L}, respectively. According to this assumption, the slit width, w, to maximally damp J_{L}, should satisfy the condition

$$w\mathrm{sinc}\left[\left(\frac{\sin\theta}{\lambda} + \alpha_{\mathrm{SPP}}\right)w\right] = 0. \tag{5}$$

The slit width for the local minimum excitation of J_{L}, $w_{\mathrm{L,m}}$, is obtained, from Eq. (5), as

$$w_{L,m} = m \Big/ \left(\frac{\sin\theta}{\lambda} + \frac{1}{\lambda_{SPP}}\right), \text{ for } m = 1, 2, \cdots. \tag{6a}$$

The slit width for the local maximum excitation of J_L, $w_{H,m}$, is obtained by

$$w_{H,m} = (m - 0.5) \Big/ \left(\frac{\sin\theta}{\lambda} + \frac{1}{\lambda_{SPP}} \right), \text{ for } m = 1, 2, \cdots. \tag{6b}$$

In the normal incidence condition, the minimum and maximum SPP excitation slit widths are given, respectively, by $w_{L,m}=m\lambda_{SPP}$ and $w_{H,m}=(m-0.5)\lambda_{SPP}$. Let us inspect the validity of the derived expectation formulas of Eqs. (6a) and (6b) by comparing the results of the RCWA and the expectations of the formulas. For this, the z-directional electric field intensity is represented as a function of the spatial variables, x, z, the slit width, w, and the incidence angle, θ, i.e., $E_z(x,z,w,\theta)$. Using the RCWA, we have calculated the z-directional electric field intensity distributions at z=50 nm, $|E_z(x, 50\text{ nm}, w, \theta)|$, for slit width values from 10 nm to 4 μm. In Figs. 5(a) and 6(a), $|E_z(x, 50\text{ nm}, w, 0°)|$ obtained for the normal backside illumination and $|E_z(x, 50\text{ nm}, w, 55°)|$ for the oblique backside illumination are displayed for comparison, respectively.

In both cases of the normal and oblique illuminations, near-periodic SPP excitation patterns for the slit width variation are observed. Let us concern the local minimum and maximum slit widths of J_L. The SPP intensity traces at the points 1.5 μm distant from the left slit edge for slit width variation for normal and oblique illuminations, $|E_z(w+1.5\text{ μm}, 50\text{ nm}, w, 0°)|$ and $|E_z(w+1.5\text{ μm}, 50\text{ nm}, w, 55°)|$, are plotted in Figs. 5(b) and 6(b), respectively. The local minimum excitation slit, $w_{L,m}$ and the local maximum excitation slit, $w_{H,m}$, obtained from Eqs. (6a) and (6b) are indicated by the blue circles and the red circles in Figs. 5(b) and 6(b). In the case of normal illumination, as seen in Fig. 5(b), the blue circles at $w_{L,m}$ are well-matched on the local minimum of the SPP intensity and the red circles at $w_{H,m}$ are also matched on the local maximum of the SPP except the second peak around w=730 nm. However, in the case of oblique illumination, as seen in Fig. 6(b), both the blue circles at $w_{L,m}$ and the red circles at $w_{H,m}$ do not match the local minimum and maximum points. This lack of validity of Eqs. (6a) and (6b) requires further refinement over the first diffraction model. From the RCWA results, we can see that the slit width producing the maximum strength of J_L is obtained by w=730 nm for normal illumination and, when the illumination angle is θ=55°, the second minimum point of J_L is observed at the same slit sample with slit width of 730 nm. The examples shown in Figs. 2 and 3 are the electric field distributions generated by the slit sample with slit width of 730 nm under normal and oblique illuminations, respectively.

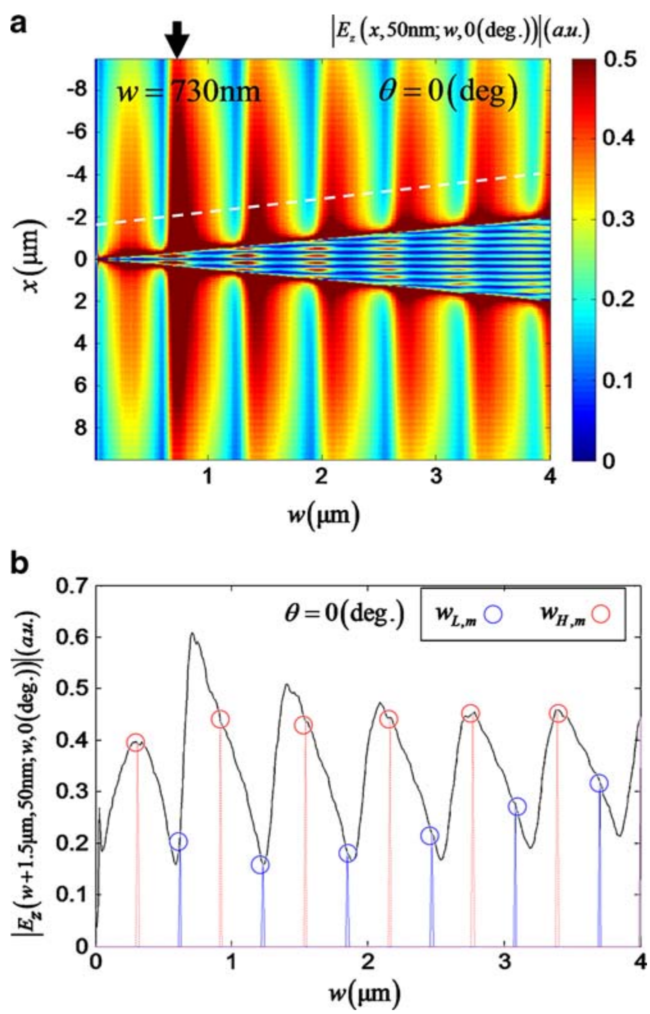

Fig. 5 **a** SPP intensity distributions at z=50 nm and for normal illumination (θ=0°), $|E_z(x,50\text{ nm},w,0°)|$ for slit width variation, **b** trace of the SPP intensity distribution along the white dashed line, $x=w+1.5$ μm, $|E_z(w+1.5\text{ μm},50\text{ nm},w,0°)|$

Next, let us find refined formulas giving correct expectation of the local minimum and maximum excitation conditions of J_L based on the second aperture diffraction model shown in Fig. 4(b). The dark triangle region in Fig. 4(b) is the effective shadow caused by the finite thickness slit wall under oblique incidence, which is referred to as the shadow effect. At the left lower edge of the slit, the incident plane wave is diffracted to generate a boundary diffraction field. Since the diffraction field cannot fill the whole space of the slit, the dark region between the left slit wall and the diffraction field region exists effectively. In reality, the optical field around the sidewall would be gradually tailored to dark. The effective shadow means that the gradually tailored optical field intensity around the sidewall is approximated by a geometric dark shadow. In Fig. 4(b), the angle between the slit wall and the dark region boundary is denoted by Ψ. When the corner angle of the triangle dark region is considered, then we

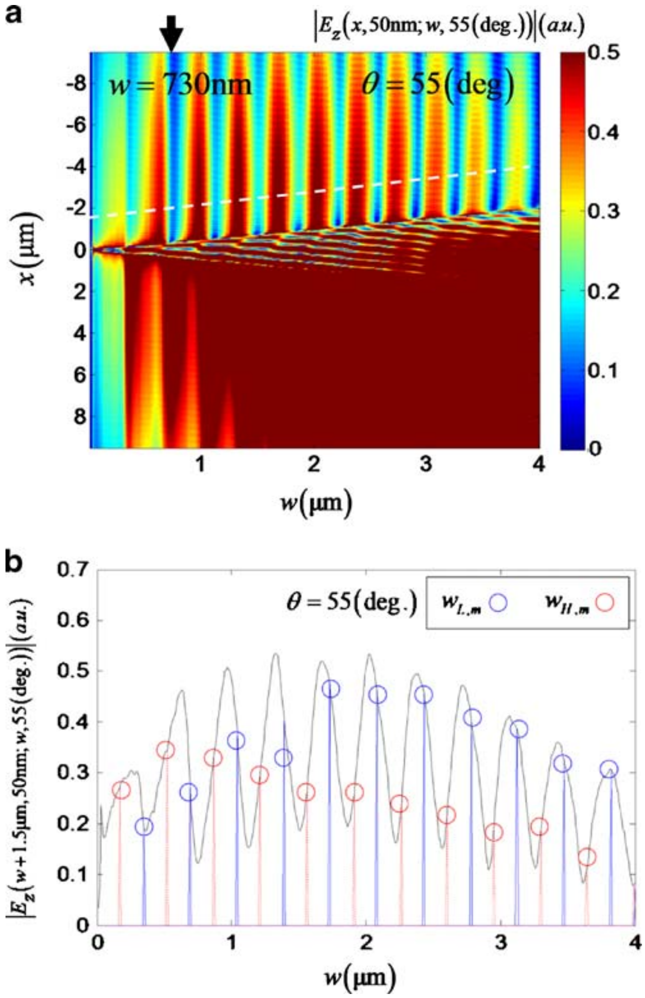

Fig. 6 **a** SPP intensity distributions at z=50 nm and for oblique illumination (θ=55°), $|E_z(x,50\ \text{nm},w,55°)|$ for slit width variation, **b** trace of the SPP intensity distribution along the white dashed line, $x=w+1.5$ μm, $|E_z(w+1.5\ \mu\text{m},50\ \text{nm},w,55°)|$

should distinguish the real slit width, $\overline{w}$, and the effective slit width, w, which is the effective width of the optical field distributed on the slit. The relationship between $\overline{w}$ and w is given by

$$\overline{w} = w + t\tan\psi. \tag{7}$$

If we consider w in the structural angular spectrum of Eq. (3), we can see that under the oblique incidence, a slightly wider real slit width $\overline{w}$ than the effective width w by the amount of $t\tan\Psi$ is necessary for invoking the effective width w. We do not know the mathematical theory that provides the exact description of the edge diffraction, while we can infer the qualitative properties intuitively and devise approximate formulas describing the corner angle Ψ from the physical intuition. This approximate mathematical fitting formula is a phenomenological expression, which is devised from a physical intuition hinted in the Sommerfeld's half-infinite diffraction problem.

The approximate relationship of Ψ and θ can be obtained from the following phenomenological assumptions; Ψ is not exactly linearly but monotonically proportional to both θ and w. For fixed $w(\theta)$, Ψ increases as $\theta(w)$ increases since the finite confinement of the slit width influences the edge diffraction. With these in mind, we take the phenomenological fitting expression between Ψ and θ as

$$\psi = [c_1 + c_2\sin(\pi(\gamma-1)/c_3)]\theta, \tag{8a}$$

where γ is defined by

$$\gamma = w(\sin\theta/\lambda + 1/\lambda_{\text{SPP}}), \tag{8b}$$

and c_1, c_2, and c_3 are the fitting parameters. For the film thickness of 300 nm, c_1, c_2, and c_3 are obtained as 0.09, 0.8 and 48, respectively. As a result, Ψ is then expressed in the form:

$$\psi = [0.09 + 0.8\sin(\pi(\gamma-1)/48)]\theta. \tag{8c}$$

The distribution of Ψ for θ and w is plotted as a slightly curved and monotonically increasing surface with increasing θ and Ψ as shown in Fig. 7(a).

We show that the three-parameter fitting formula of Eq. (8a) can adjust the mismatch errors (see Figs. 5 and 6) of the classical scalar diffraction model over whole ranges of both θ and w. The width of the shadow region in Fig. 4(b), $\Delta w(\theta, \gamma, t)$ is given by

$$\Delta w(\theta,\gamma,t) = t\tan\psi. \tag{9}$$

The real slit width, $w_{L,m}$ for the minimum excitation condition of J_L is given by the sum of the effective slit width, $w_{L,m}$, and the shadow region width, $\Delta w(\theta, \gamma, t)$, as

$$\overline{w}_{L,m} = w_{L,m} + \Delta w(\theta, m, t), \tag{10a}$$

where it is noted that γ becomes m from Eq. (6a) at the local minimum SPP excitation condition. Also, with the shadow effect considered, the real slit width, $\overline{w}_{H,m}$, for the maximum SPP excitation condition is obtained as

$$\overline{w}_{H,m} = w_{H,m} + \Delta w(\theta, m-0.5, t). \tag{10b}$$

The modified local minimum and maximum SPP excitation slit widths, $\overline{w}_{L,m}$ and $\overline{w}_{H,m}$, are plotted in Fig. 7(b) by the blue circles and red circles, respectively. As seen in Fig. 7(b), the blue circles at $\overline{w}_{L,m}$ are well-matched on the local minimum of the SPP and the red circles at $\overline{w}_{H,m}$ are also matched on the local maximum. To examine the derived formulas, the distributions of $w_{L,m}$ and $\overline{w}_{L,m}$ are compared on the map of the SPP intensity distribution, $|E_z(w+1.5\ \mu\text{m},50\ \text{nm},w,\theta)|$, calculated for slit widths from 10 nm to 4 μm and illumination angles from 0° to 80°. In Fig. 8(a), the local minimum slit widths, $w_{L,m}$, for incidence angles θ are compared with the local minimum points in $|E_z(w+1.5\ \mu\text{m},50\ \text{nm},w,\theta)|$ analyzed by the RCWA. Significant errors are observed as expected in Fig. 6(b). In Fig. 8(b), the local minimum slit widths, $\overline{w}_{L,m}$,

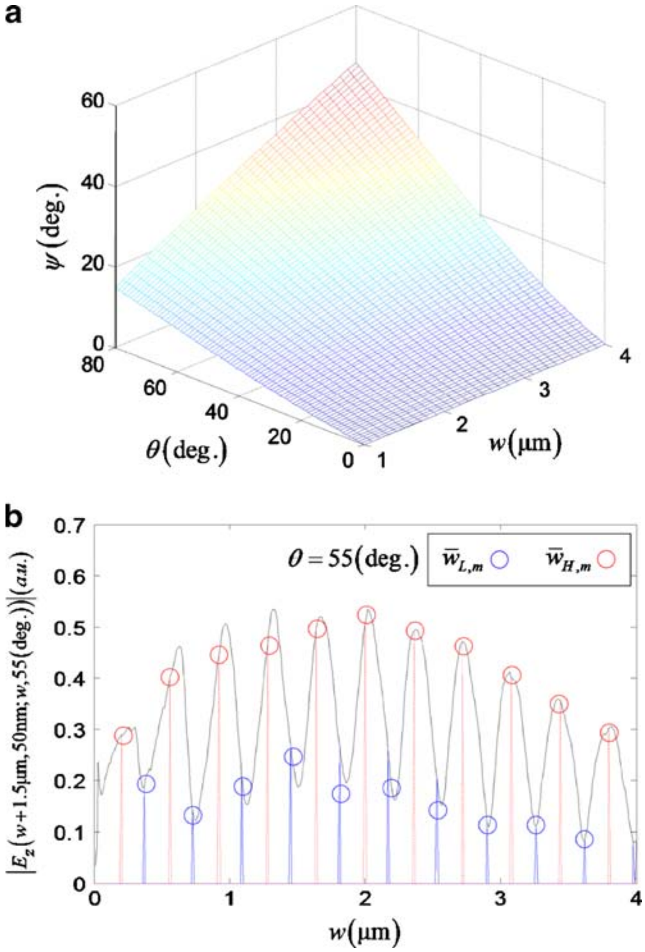

Fig. 7 **a** Distribution of the approximately modeled edge diffraction angle, Ψ, for θ and w variations, **b** trace of the SPP intensity distribution along the line $x = w + 1.5\mu$m, $|E_z(w + 1.5\mu\text{m}, 50\text{nm}, w, 55°)|$

derived from the second diffraction model are compared with the local minimum points in $|E_z(w{+}1.5\ \mu\text{m}, 50\ \text{nm}, w, \theta)|$ analyzed by the RCWA. It is seen that the $\overline{w}_{L,m}$ is well-matched to the local minimum points in whole incidence angle range.

Although a phenomenological approach with the sidewall shadow effect instead of finding the exact solution of the Maxwell equations is adopted in this paper, it has been shown that the angular spectrum based scalar diffraction theory from the aperture diffraction model with the shadow effect provides a reasonable interpretation and explicit conditions of the unidirectional SPP excitation.

Conclusion

In conclusion, it has been shown that the oblique backside illumination on a single slit induces the unidirectional SPP excitation. The diffraction model with the shadow effect induced by the finite thickness slit sidewall is proposed, and the unidirectional SPP excitation condition is derived from the diffraction model with a phenomenological approximate fitting formula on the shadow region. The unidirectional surface plasmon excitation occurs when the zero point of the angular spectrum of the rectangle function with the effective slit width matches to the eigen spatial-frequency of the SPP, α_{SPP}. The validity of the devised analytic formula on the unidirectional SPP excitation condition has been confirmed with rigorous vectorial electromagnetic simulations. The unidirectional SPP excitation with oblique illumination is quite simple, so it would be useful for various applications and research problems requiring efficient SPP excitation.

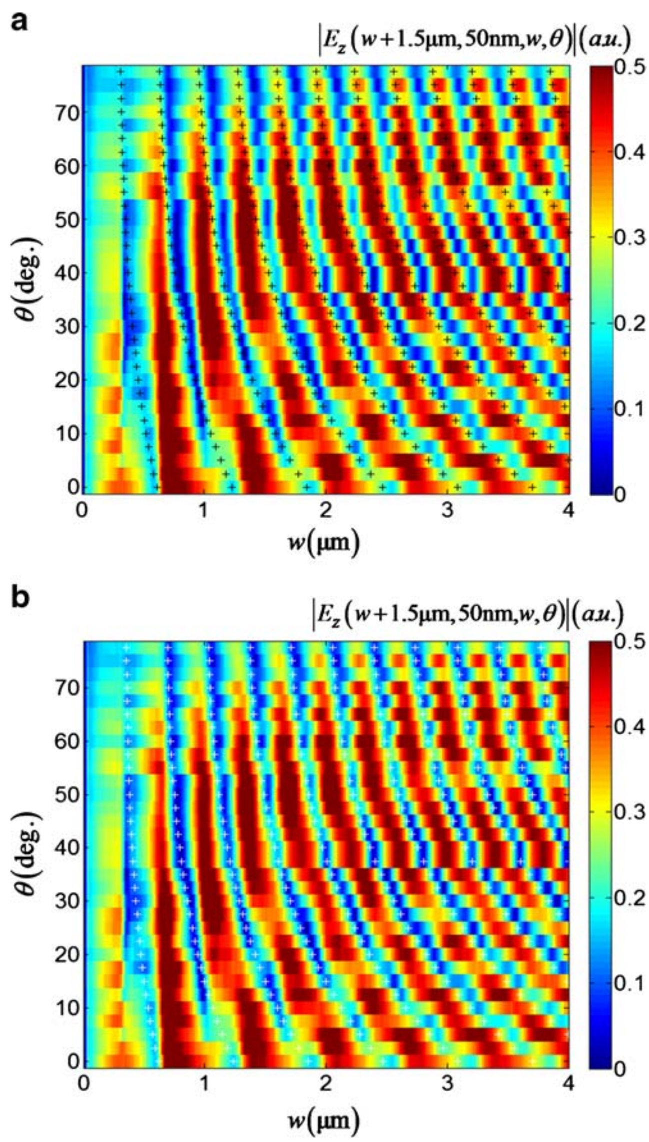

Fig. 8 **a** Plot of the local minimum SPP excitation slit width, $w_{L,m}$ (black +) on the distribution $|E_z(w + 1.5\mu\text{m}, 50\text{nm}, w, \theta)|$ and **b** plot of the local minimum SPP excitation slit width, $\overline{w}_{L,m}$ (white +) obtained by $\overline{w}_{L,m} = w_{L,m} + \Delta w(\theta, m, 300\text{nm})$ on the distribution $|E_z(w + 1.5\mu\text{m}, 50\text{nm}, w, \theta)|$

Acknowledgment This work was supported by Ministry of Education, Science and Technology of Korea and Korea Science and Engineering Foundation through the Creative Research Initiatives Program (Active Plasmonics Application Systems).

References

1. Barnes WL, Dereux A, Ebbesen TW (2003) Surface plasmon subwavelength optics. Nature 424:824–830. doi:10.1038/nature01937
2. Ozbay E (2006) Plasmonics: merging photonics and electronics at nanoscale dimensions. Science 311:189–193. doi:10.1126/science.1114849
3. Takahara J, Kobayashi T (2004) Low-dimensional optical waves and nano-optical circuits. Opt Photon News 15:54–59. doi:10.1364/OPN.15.10.000054
4. Novotny L, Hecht B (2006) Principles of nano-optics. Cambridge University Press, Cambridge
5. Lopez-Tejeria F, Rodrigo SG, Martin-Moreno L, Garcia-Vidal FJ, Devaux E, Ebbesen TW, Krenn JR, Padko IP, Bozhevolnyi SI, Gonzalez MU, Weeber JC, Dereux A (2007) Efficient unidirectional nanoslit couplers for surface plasmons. Nat Phys 3:324–328. doi:10.1038/nphys584
6. Bonod N, Popov E, Li L, Chernov B (2007) Unidirectional excitation of surface plasmons by slanted gratings. Opt Express 15:11427–11432. doi:10.1364/OE.15.011427
7. Lalanne P, Hugonin JP, Roider JC (2005) Theory of surface plasmon generation at nanoslit apertures. Phys Rev Lett 95:263902. doi:10.1103/PhysRevLett.95.263902
8. Kihm HW, Lee KG, Kim DS, Kang JH, Park Q-H (2008) Control of surface plasmon generation efficiency by slit-width tuning. Appl Phys Lett 92:05115. doi:10.1063/1.2840675
9. Kim S, Kim H, Lim Y, Lee B (2007) Off-axis directional beaming of optical field diffracted by a single subwavelength metal slit with asymmetric dielectric structure surface gratings. Appl Phys Lett 90:051113. doi:10.1063/1.2437730
10. Kim S, Lim Y, Kim H, Park J, Lee B (2008) Optical beam focusing by a single subwavelength metal slit surrounded by chirped dielectric surface gratings. Appl Phys Lett 92:013103. doi:10.1063/1.2828716
11. Kim H, Lee I-M, Lee B (2007) Extended scattering-matrix method for efficient full parallel implementation of rigorous coupled-wave analysis. J Opt Soc Am A 24:2313–2327. doi:10.1364/JOSAA.24.002313
12. Born M, Wolf E (1999) Two-Dimensional Diffraction of a Plane Wave by a Half-Plane Sec 11.5 in Principle of Optics 7th ed. Cambridge University Press